

Electronic structure calculations on the C₄ cluster

H. Massó and M. L. Senent^{a),b)}*Departamento de Astrofísica Molecular e Infrarroja, Instituto de Estructura de la Materia, CSIC, Serrano 121, Madrid 28006, Spain*P. Rosmus and M. Hochlaf^{a),c)}*Theoretical Chemistry Group, University of Marne-la-Vallée, Champs sur Marne, F-77454 Marne-la-Vallée, Cedex 2, France*

(Received 15 February 2006; accepted 23 February 2006; published online 16 June 2006)

The ground and the electronically excited states of the C₄ radical are studied using interaction configuration methods and large basis sets. Apart from the known isomers [*l*-C₄(X³Σ_g⁻) and *r*-C₄(X¹A_g)], it is found that the ground singlet surface has two other stationary points: *s*-C₄(X¹A_g) and *d*-C₄(X¹A₁). The *d*-C₄ form is the third isomer of this cluster. The isomerization pathways from one form to the other show that deep potential wells are separating each minimum. Multireference configuration interaction studies of the electronic excited states reveal a high density of electronic states of these species in the 0–2 eV energy ranges. The high rovibrational levels of *l*-C₄(³Σ_u⁻) undergo predissociation processes via spin-orbit interactions with the neighboring ⁵Σ_g⁺ state. © 2006 American Institute of Physics. [DOI: 10.1063/1.2187972]

I. INTRODUCTION

C_{*n*} carbon chains play an important role in the interstellar chemistry of carbon-rich evolved stars as stable species or chemical intermediates. Because of their astrophysical significance and chemical importance, they have been subject of extensive investigations based on high resolution spectroscopy or high level *ab initio* calculations. These species have been proposed by Douglas¹ as possible constituent of the diffuse interstellar bands (DIBs). The review of Van Orden and Saykally² gives a description of previous studies performed on the C_{*n*} radicals during the past. From this review, it appears that short carbon chains (*n* < 10) are not well characterized experimentally. Some C_{*n*} radicals present high reactivity, which makes their experimental observations difficult. For many carbon clusters only *ab initio* theoretical data are available. The existence of several isomers and the large density of electronic states even at low internal energy range make their theoretical computations difficult. Especially, *ab initio* studies of C_{*n*} radicals with an even number of atoms present a challenging problem due to the existence of various isomers with comparable stability. Many aspects involving structure and spectroscopic properties are still controversial.

The present work treats one of this carbon clusters with some intriguing features: the C₄ radical. Two isomers of similar stabilities, one linear (*l*-C₄) and one rhombic (*r*-C₄), have been observed experimentally. Recently, the group in Madrid³ has detected in SgrB2, IRC+10216, CRL 2688, and NGC 7027 with the *Infrared Space Observatory* a pattern of bands at 57 μm (174 cm⁻¹), the assignment of which to the fundamental transitions of the ν₅ bending of *l*-C₄ was suggested. Evidence for *r*-C₄ has been obtained by the Coulomb

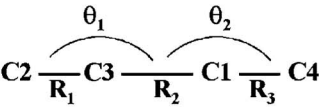
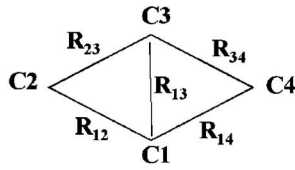
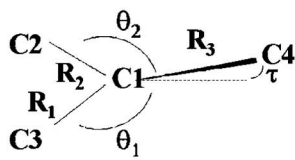
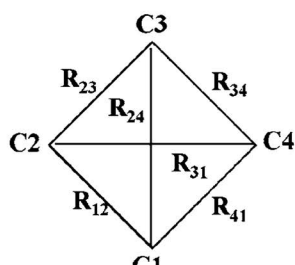
explosion imaging technique that revealed also the existence of a third tetrahedral isomer.^{4,5} The first observation of linear C₄ performed with electronic spin resonance spectroscopy of carbon clusters trapped in solid Ne and Ar matrices⁶ led to a controversy concerning the radical structure. Two possible configurations, cumulenic and acetylenic, were postulated. A near-linear bent structure has been proposed as possible origin of the line splitting observed in electron spin resonance experiments.^{7,8} Gas phase high resolution spectroscopy confirmed a linear structure.⁹ Theoretically, previous works have found the cumulenic structure (of ³Σ_g⁻ symmetry species) as the most stable form of *l*-C₄.¹⁰ Nevertheless, the absolute relative energy position of *l*-C₄/*r*-C₄ is not yet established and the isomerization pathway between them is not known.

Concerning the electronic excited states of *l*-C₄, two states, the ¹Δ_g and ¹Σ_g⁺ states, arising from the π² configurations as the X³Σ_g⁻, were computed by Liang and Schaeffer III.¹⁰ They are predicted to lie at 0.332 and 0.93 eV above the cumulenic structure. For *r*-C₄, Mühlhäuser *et al.*¹¹ have located several singlet states in the 0–5 eV internal energy range. Experimentally, numerous accurate data on these electronic states have been published by Maier and co-workers^{12–16} and Jungen and Xu¹⁷ using photoelectron spectroscopy and by the absorption spectra of C₄ in cold matrices. Xu *et al.*¹⁸ reported vertical excitation energies for *l*-C₄ from photoelectron spectroscopy and *ab initio* calculations.

Here, we are treating the C₄ carbon cluster using large *ab initio* computations. Specifically, the stationary points of the ground potential energy surfaces of the C₄ carbon cluster and of its lowest electronic states of singlet, triplet, and quintet spin multiplicities are investigated using configuration interaction approaches. We have also considered the intramolecular isomerization pathways.

^{a)}Authors to whom correspondence should be addressed.^{b)}Electronic mail: senent@damir.iem.csic.es^{c)}Electronic mail: hochlaf@univ-mlv.fr

TABLE I. Structural parameters (distances R_i in Å, angles in degrees) and total energies (E in hartrees) of stationary points of C_4 . E_R (in cm^{-1}) is the relative energy with respect to the $l\text{-C}_4(X^3\Sigma_g^-)$ equilibrium minimum.

		cc-pVQZ/RCCSD-T ^a	cc-pVQZ/CASSCF ^a	cc-pVTZ/MRCI+Q ^a	
	$l\text{-C}_4(D_{\infty h})(X^3\Sigma_g^-)$	$R_1=R_3^b$	1.293 6	1.293 8	1.296 0
		R_2^c	1.313 6	1.299 6	1.316 7
		E	-151.827 478	-151.376 368	-151.761 481 ^d
	$r\text{-C}_4(D_{2h})(X^1A_g)$	R_{31}^e	1.512	1.529 3	1.520 4
		R_{12}^f	1.448 3	1.443 7	1.441 4
		E (a.u.)	-151.830 061	-151.365 604	-151.723 128 ^d
		E_R^b	-567	2 362	
	$d\text{-C}_4(C_{2v})(X^1A_1)$	$R_1=R_2$	1.450 1	1.464 8	1.452 6
		R_3	1.338 8	1.318 2	1.339 8
		$\theta_1=\theta_2$	151.1	152.1	151.5
		E	-151.786 082	-151.325 121	-151.675 966 ^d
		E_R	9 085	11 247	
	$s\text{-C}_4(D_{4h})(X^1A_g)$	R_{12}	1.444 1	1.431 8	
		E	-151.716 017	-151.229 780	
		E_R	24 463	32 172	

^aActive spaces containing 12 π orbitals. Eight orbitals (four core orbitals and four σ valence orbitals) have been considered doubly occupied in all the configurations, but they have been optimized.

^bPrevious results: 1.292 Å [5s4p1d/MBPT(4)] (Ref. 19) and 1.2907 Å [336 cGTOs/RCCSD(T)] (Ref. 29).

^cPrevious results: 1.314 Å [5s4p1d/MBPT(4)] (Ref. 19) and 1.3098 Å [336 cGTOs/RCCSD(T)] (Ref. 29).

^dMRCI value.

^ePrevious results: 1.5138 Å [5s4p1d/MBPT(4)] (Ref. 19) and 1.502 Å [vtz/CCSD(T)] (Ref. 30).

^fPrevious results: 1.423 Å [5s4p1d/MBPT(4)] (Ref. 19) and 1.442 Å [vtz/CCSD(T)] (Ref. 30).

II. MOLECULAR STRUCTURE OF C_4

It is well established² that the C_4 radical has two isomers: one linear ($l\text{-C}_4$) of $D_{\infty h}$ symmetry and one rhombic ($r\text{-C}_4$) of D_{2h} symmetry. Our computations confirm that the electronic ground state of $l\text{-C}_4$ is the $X^3\Sigma_g^-$ state resulting from the π^2 electronic configuration. The ground electronic state of $r\text{-C}_4$ is the X^1A_g . Table I lists the characteristics of both linear and rhombic forms including their internuclear distances (in angstroms) and their in-plane angles (in degrees). It is worth noting that the two diagonals of $r\text{-C}_4$ show different lengths and that only the shorter one can be considered as a real intramolecular bond.

The relative energy position of these two forms is not definitely established in the literature. Watts *et al.*¹⁹ have reported an energy difference between isomers that varies

between -575 and [cc-pVQZ/UHF-CCSD(T)] 1420 cm^{-1} (G[542]/MRCI), relative to the $l\text{-C}_4(X^3\Sigma_g^-)$ minimum. Here, preliminary cc-pVTZ/B3LYP density functional calculations were used to explore the ground six-dimensional (6D) potential energy surfaces (PESs). Then, more accurate results were obtained with the coupled cluster technique²⁰ (RCCSD-T) and complete active space self-consistent field²¹ (CASSCF) approach followed by the internally contracted multireference configuration interaction (MRCI) method,^{22,23} implemented in MOLPRO (Ref. 24) and three different basis sets (cc-pVTZ, aug-cc-pVTZ, and cc-pVQZ).²⁵ For the CASSCF calculations, various different active spaces selected using orbital occupancies and symmetries have been explored. In MRCI calculations, all configurations having a weight greater than 0.03 in the configuration interaction (CI) expansion of the CASSCF wave functions were taken as reference. All valence electrons were correlated.

In Table I the total electronic energies, the isomers' relative energies, and the structural parameters of the stationary points of C₄ considered in the present work are given. Our coupled cluster results lead to the rhombic form as the most stable structure, whereas the CASSCF calculations yield the linear isomer as the most stable isomer (cf. Table I). Different calculations of this relative energy using either RCCSD-T or CASSCF and different basis sets with increasing size show that the size of the basis set is not that crucial and that correlation energy is more important. This quantity is calculated to be -262 , -405 , and -567 cm⁻¹ at the cc-pVTZ/RCCSD-T, aug-cc-pVTZ/RCCSD-T, and cc-pVQZ/RCCSD-T levels of theory, respectively. The corresponding calculations with CASSCF give 2961, 1908, and 2362 cm⁻¹ using cc-pVTZ, aug-cc-pVTZ, and cc-pVQZ basis sets. In these CASSCF calculations, the active space comprised all the 12π orbitals, but the four lowest σ valence orbitals have been kept doubly occupied. Accordingly, a final statement about the global minimum of C₄ is hardly possible since these energy differences are within the error bars of the computational methods used here, albeit they are already rather extensive ones. This is in accordance with previous discussions in the literature pointing out difficulties of computations for even carbon atoms clusters. Nevertheless, a general trend can be stated: multiconfigurational calculations support the assumption that *l*-C₄ is the most stable form.

Table I shows that two additional stationary points on the lowest C₄ potential energy function (PEF) exist: *d*-C₄ and *s*-C₄. They are located at 1.13 and 3.03 eV above the linear minimum using cc-pVQZ/RCCSD-T and cc-pVQZ/UCCSD-T calculations. These two structures can be important intermediates during astrophysical reactions involving carbon chains and of the isomer interconversion processes. The *d*-C₄ ground state is a singlet with a planar C_{2v} structure, in which three carbon atoms are attached to the same central carbon atom. In the present paper, we describe it as a local minimum of low stability. The cyclic one, *s*-C₄, has D_{4h} symmetry and a singlet ground electronic state of ¹A_g symmetry species. It seems reasonable to consider it as the top of a barrier restricting the interconversion process of the two equivalent conformers of the rhombic isomer (one of them with R₂₄ > R₁₃ and the second one with R₁₃ > R₂₄). It has been found unstable [E_R = 4.0 eV (CASSCF) and 3.03 eV (UCCSD(T))] lying over the lowest singlet and triplet states of *r*-C₄. Recently, a similar situation was found for the B₄ cluster,²⁶ except that the D_{4h} transition state is lying only at 248.2 cm⁻¹ favoring interconversion processes to occur via tunneling through this potential barrier. For C₄, it is unlikely that such effect takes place for the low lying rovibrational levels of *r*-C₄ because of the large potential energy barrier separating both forms.

The *d*-C₄ (X ¹A₁) isomer is a good candidate for the third isomer of C₄ not characterized yet but detected in the Coulomb explosion experiments.⁵ For that reason, more attention was paid for obtaining the structural parameters of this isomer. *d*-C₄ appears to be a minimum. Interaction configuration computations performed with different active spaces produce results either with all the harmonic frequencies positive (i.e., a local minimum) or with one of the fundamentals

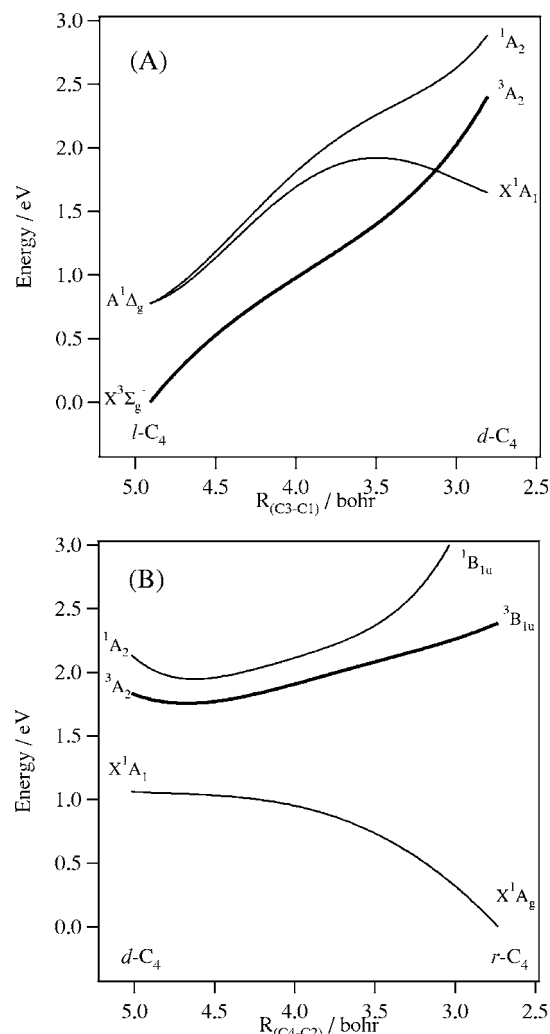
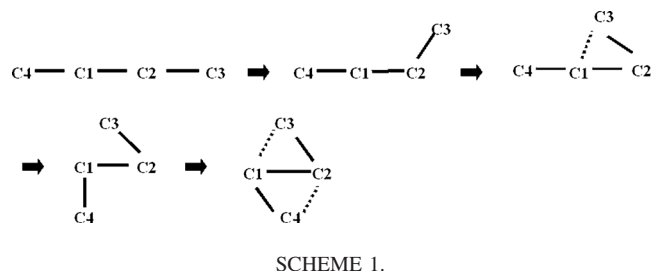


FIG. 1. CASSCF one-dimensional cuts on the 6D PEFs of the lowest triplet (³A₂) and the two singlet (¹A₁ and ¹A₂) electronic states of *d*-C₄ along the C₁-C₃ distance (in A) and the C₄-C₂ distance (in B) corresponding to the *l*-C₄ → *d*-C₄ and the *d*-C₄ → *r*-C₄ isomerization processes, respectively. See text for more details.

slightly negative (i.e., transition state). At lower levels of theory, *d*-C₄ shows a slightly distorted C_{2v} structure. With our best wave function, all the frequencies are found positive, for instance, preliminary force field calculations performed at the MRCI level give the following harmonic positive frequencies: ω₁ = 1642(a₁), ω₂ = 1395(a₁), ω₃ = 842(a₁), ω₄ = 397(b₁), ω₅ = 791(b₂), and ω₆ = 182(b₂) (all values are in cm⁻¹). A definitive theoretical characterization of *d*-C₄ requires very highly correlated methods. In addition, our calculations converge always to a planar geometry, whereas the detected one is nonplanar.⁵ A coupling of two vibrational modes (the two asymmetric modes R₁-R₂ and θ₁-θ₂) should permit the transformation leading to the two rhombic forms discussed above. The *d*-C₄(X ¹A_g) form is located well below *s*-C₄ and it is computed to be 1.1 eV (cc-pVQZ/RCCSD-T) and 1.4 eV (cc-pVQZ/CASSCF) higher than the linear form. The *d*-C₄ (X ¹A₁) structure exists below the lowest electronically excited singlet of *r*-C₄ (cf. *infra*).

III. ISOMERIZATION PROCESSES

Figure 1 depicts the one-dimensional cuts on the 6D PESs of the lowest triplet (3A_2 or $^3B_{1u}$) and two lowest singlet (1A_1 and 1A_2 or 1A_g and $^1B_{1u}$) states of C_4 along the isomerization scheme 1:²⁷



These calculations were performed at the cc-pVTZ/CASSCF level of theory (comprised of all the 12π orbitals in the active space). We would like to point out that the curves in Fig. 1 do not correspond to the minimal energy path for these isomerization processes, but they are computed to give an insight into the evolution of the 6D PESs when l - C_4 is transforming into r - C_4 [Fig. 1(a)] and then to d - C_4 [Fig. 1(b)].

The curves for the singlet in Fig. 1(a) correspond to the two components of the doubly degenerate $^1\Delta_g$ state (for instance, 1A_2 and X^1A_1) and the curve for the triplet is for the $X^3\Sigma_g^-$ state of l - C_4 transforming into d - C_4 . This figure shows that l - $C_4(^1\Delta)$ splits in energy into two Renner-Teller components. Figure 1(a) reveals the existence of a crossing between the triplet (3A_2) and the lowest singlet (X^1A_1) for C_3 - C_1 distances of about 3.4 bohrs, where spin-orbit conversion processes can take place. In Fig. 1(b), the energy variation corresponding to the lowest electronic states is represented as a function of the C_4 - C_2 coordinate for the d - $C_4 \rightarrow r$ - C_4 isomerization process. Local minima are calculated along this coordinate for the $^3B_{1u}$, 1A_g , and $^1B_{1u}$ electronic states. These local minima may correspond to transient species of C_4 and can be populated during the reactive collisions involving C_4 . Finally, it is worth noting that the cuts of the lowest singlet and triplet states go up in energy by decreasing the C_1 - C_3 distance, resulting in deep potential wells (more than 4000 cm^{-1}) around each potential minimum. This should allow to study experimentally and theoretically each isomer.²⁸

IV. ON THE ELECTRONIC EXCITED STATES OF C_4

Figure 2 presents the collinear CASSCF one-dimensional cuts of the 6D PESs of the lowest electronic states of l - C_4 of singlet [Fig. 2(a)] triplet [Fig. 2(b)], and quintet [Fig. 2(c)] spin multiplicities. These cuts are shown along the middle CC stretch (R_{CC}), where both external CC bonds are kept fixed at 2.45 bohrs. In Table II, the vertical excitation energies calculated in the present paper are compared with the experimental values. The papers of Maier and co-workers¹²⁻¹⁶ provide low vertical energies for the lowest states. Generally, our MRCI vertical excitation energies agree relatively well with the experimental T_0 determinations

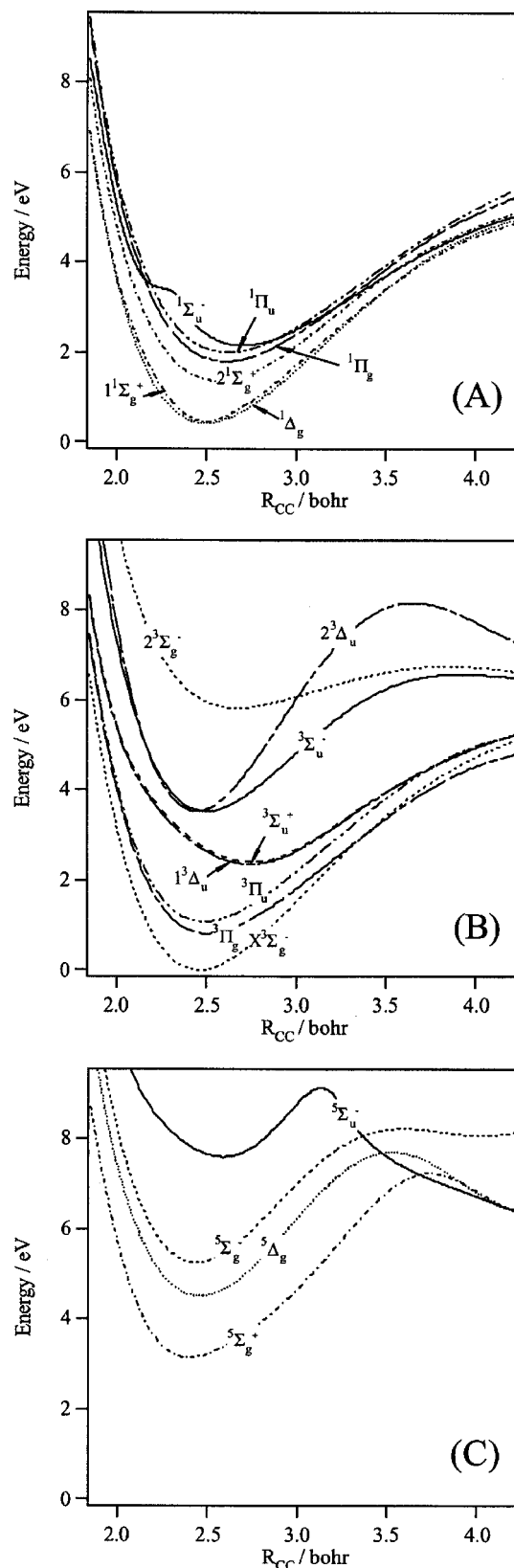


FIG. 2. Collinear CASSCF one-dimensional cuts of the lowest singlet (A), triplet (B), and quintet (C) electronic states of l - C_4 along the middle CC stretch (R_{CC}). The external CC bonds are kept fixed at 2.45 bohrs. These curves are given with respect to the minimum of l - $C_4(X^3\Sigma_g^-)$.

of Refs. 15, 16, 18, and 31 assuming that our values will be decreased if one considers the relaxation of all six internal coordinates. For instance, the first excited state of l - C_4 (i.e.,

TABLE II. Dominant electronic configurations and cc-pVTZ/MRCI vertical excitation energies (T , in eV) of the lowest electronic states of $I-C_4$.

State	T^a (CASSCF)	T^a (MRCI)	T_0^a (Expt.)	Electronic configuration
$X^3\Sigma_g^-$	0 ^a	0 ^c	0	$(3\sigma_g)^2(3\sigma_u)^2(4\sigma_g)^2(1\pi_u)^4(1\pi_g)^2$
$1^1\Delta_g$	0.43	0.44	0.33 ^{d,e}	$(3\sigma_g)^2(3\sigma_u)^2(4\sigma_g)^2(1\pi_u)^4(1\pi_g)^2$
$1^1\Sigma_g^+$	0.47	0.61	0.50 ^e	$(3\sigma_g)^2(3\sigma_u)^2(4\sigma_g)^2(1\pi_u)^4(1\pi_g)^2$
$3^1\Pi_g$	0.82	1.09	0.82 ^e	$(3\sigma_g)^2(3\sigma_u)^2(4\sigma_g)^1(1\pi_u)^4(1\pi_g)^3$
$3^1\Pi_u$	1.08	1.37	0.93 ^f	$(3\sigma_g)^2(3\sigma_u)^1(4\sigma_g)^2(1\pi_u)^4(1\pi_g)^3$
$2^1\Sigma_g^+$	1.43	1.86		$(3\sigma_g)^2(3\sigma_u)^2(4\sigma_g)^0(1\pi_u)^4(1\pi_g)^4$
$1^1\Pi_g$	1.92	1.93	1.41 ^e	$(3\sigma_g)^2(3\sigma_u)^2(4\sigma_g)^1(1\pi_u)^4(1\pi_g)^3$
$1^1\Pi_u$	2.14	2.20	1.16 ^{e,g}	$(3\sigma_g)^2(3\sigma_u)^1(4\sigma_g)^2(1\pi_u)^4(1\pi_g)^3$
$1^1\Sigma_u^-$	2.51	2.61		$(3\sigma_g)^2(3\sigma_u)^2(4\sigma_g)^2(1\pi_u)^3(1\pi_g)^3$
$1^3\Delta_u$	2.72	2.82		$(3\sigma_g)^2(3\sigma_u)^2(4\sigma_g)^2(1\pi_u)^3(1\pi_g)^3$
$3^1\Sigma_u^+$	2.78	2.84		$(3\sigma_g)^2(3\sigma_u)^2(4\sigma_g)^2(1\pi_u)^3(1\pi_g)^3$
$5^1\Sigma_g^+$	3.18	3.82		$(3\sigma_g)^2(3\sigma_u)^1(4\sigma_g)^1(1\pi_u)^4(1\pi_g)^3(2\pi_u)^1$
$2^3\Delta_u$	3.53	3.56		$(3\sigma_g)^2(3\sigma_u)^2(4\sigma_g)^2(1\pi_u)^4(1\pi_g)^1(2\pi_u)^1$
$3^1\Sigma_u^-$	3.53	3.74	3.27 ^f 3.26 ^h	$(3\sigma_g)^2(3\sigma_u)^2(4\sigma_g)^2(1\pi_u)^3(1\pi_g)^3$
$5^1\Delta_g$	4.51	4.79		$(3\sigma_g)^2(3\sigma_u)^1(4\sigma_g)^1(1\pi_u)^4(1\pi_g)^3(2\pi_u)^1$
$5^1\Sigma_g^-$	5.26	5.55		$(3\sigma_g)^2(3\sigma_u)^1(4\sigma_g)^1(1\pi_u)^4(1\pi_g)^3(2\pi_u)^1$
$2^3\Sigma_g^-$	6.03	6.11		$(3\sigma_g)^2(3\sigma_u)^2(4\sigma_g)^2(1\pi_u)^3(1\pi_g)^2(2\pi_u)^1$
$5^1\Sigma_u^-$	7.70	7.98		$(3\sigma_g)^2(3\sigma_u)^1(4\sigma_g)^1(1\pi_u)^3(1\pi_g)^4(2\pi_u)^1$

^aGiven relative to $I-C_4(X^3\Sigma_g^-)$.^bTotal CASSCF energy = -151.379 361 6E_h.^cTotal MRCI energy = -151.761 480 67E_h.^dReference 31.^eReference 18.^fReference 16.^gSee text for detailed discussion.^hReference 15.TABLE III. Dominant electronic configurations and cc-pVTZ/MRCI vertical excitation energies (T , in eV) of the lowest electronic states of $r-C_4$.

State	T^a (MRCI) ^b	T^a (MRCI) ^c	Electronic configuration
X^1A_g	0 ^d	0 ^d	$(1b_{1g})^2(1b_{1u})^2(3b_{3u})^2(5a_g)^2$
3^1B_{1u}	1.04		$(1b_{1g})^2(1b_{1u})^2(3b_{3u})^1(5a_g)^2(1b_{2g})^1$
3^1B_{2g}	1.94		$(1b_{1g})^2(1b_{1u})^2(3b_{3u})^2(5a_g)^1(1b_{2g})^1$
1^1B_{1u}	2.27	2.14	$(1b_{1g})^2(1b_{1u})^2(3b_{3u})^1(5a_g)^2(1b_{2g})^1$
1^1B_{2g}	2.54	2.23	$(1b_{1g})^2(1b_{1u})^2(3b_{3u})^2(5a_g)^1(1b_{2g})^1$
1^3B_{3g}	3.12		$(1b_{1g})^2(1b_{1u})^2(3b_{3u})^2(5a_g)^1(1b_{2g})(1b_{3g})^1$
2^1A_g	3.41	3.45	$(1b_{1g})^2(1b_{1u})^2(3b_{3u})(5a_g)^2(1b_{2g})^2$
3^1B_{3u}	3.71		$(1b_{1g})^2(1b_{1u})^1(3b_{3u})^2(5a_g)^1$
1^1A_u	4.07	3.95	$(1b_{1g})^2(1b_{1u})^2(3b_{3u})^1(5a_g)^2(1b_{3g})^1$
3^1A_u	4.13		$(1b_{1g})^2(1b_{1u})^2(3b_{3u})^0(5a_g)^2(1b_{2g})^1(3b_{2u})^1$
5^1B_{2u}	4.2		$(1b_{1g})^2(1b_{1u})^2(3b_{3u})^1(5a_g)^1(1b_{2g})^1(1b_{3g})^1$
1^1B_{2u}	4.67	3.95, 6.59	$(1b_{1g})^2(1b_{1u})^2(3b_{3u})^1(5a_g)^1(1b_{2g})^1(1b_{3g})^1$
1^1B_{3g}	4.76	4.36	$(1b_{1g})^2(1b_{1u})^2(3b_{3u})^2(5a_g)^1(1b_{3g})^1$
3^1B_{2u}	4.84		$(1b_{1g})^2(1b_{1u})^2(3b_{3u})^2(5a_g)^1(3b_{2u})^1$
2^1B_{3g}	5.17	5.17	$(1b_{1g})^1(1b_{1u})^2(3b_{3u})^2(5a_g)^2(1b_{2g})^1(1b_{3g})^1$
1^1B_{3u}	5.23	4.61	$(1b_{1g})^2(1b_{1u})^2(3b_{3u})^1(5a_g)^1(1b_{2g})^2$
1^1B_{1g}	5.33	4.76	$(1b_{1g})^2(1b_{1u})^2(3b_{3u})^2(5a_g)^1(1b_{2g})^1$
2^3B_{2u}	5.35		$(1b_{1g})^2(1b_{1u})^2(3b_{3u})^2(5a_g)^1(3b_{2u})^1$
5^1B_{3g}	5.36		$(1b_{1g})^2(1b_{1u})^1(3b_{3u})^2(5a_g)^1(1b_{2g})^1(1b_{3g})^1(3b_{2u})^1$

^aGiven relative to X^1A_g .^bThis work.^cReference 11.^dTotal MRCI energy: -151.723 128E_h.

TABLE IV. Dominant electronic configurations and MRCI vertical excitation energies (T_v in eV) of the lowest electronic states of $d\text{-C}_4$ (X^1A_1). The cc-pVTZ basis set is used for these calculations.

State	Electronic configuration	T_v^a
X^1A_1	$(7a_1)^2(1b_1)^2(8a_1)^2(3b_2)^2$	0.0 ^b
3A_2	$(7a_1)^2(1b_1)^2(8a_1)^2(2b_2)^1(2b_1)^1$	0.40
3B_1	$(7a_1)^2(1b_1)^2(8a_1)^1(2b_2)^2(2b_1)^1$	0.64
1B_1	$(7a_1)^2(1b_1)^2(8a_1)^1(2b_2)^2(2b_1)^1$	0.86
1A_2	$(7a_1)^2(1b_1)^2(8a_1)^2(2b_2)^1(2b_1)^1$	1.01

^aGiven relative to $d\text{-C}_4(X^1A_1)$.

^bTotal MRCI energy: $-151.675\,966E_h$.

$^1\Delta_g$) has been observed at 0.33 eV (Ref. 18) in close agreement with our computed value of 0.44 eV. Nevertheless, the situation is quite surprising for the $^1\Pi_u$ state, which is located at 2.20 eV at the MRCI level of theory and attributed to the peak at 1.16 eV in the photoelectronic study of Xu *et al.*¹⁸ These authors claim that this attribution was found “reasonable but tentative.” Here, we do not assign the photoelectron (PES) peak at 1.16 eV to the $^1\Pi_u$ state since the errors are out of the range of the accuracy of our largest computations. This peak could be associated in the experimental spectra to vibrational excitations of the lower electronic states of C_4 .

The electronic excited states of the nonlinear isomers of C_4 are almost unknown. To our knowledge, no experimental data are available, although few papers have predicted electronic excited states for the rhombic form.¹¹ In Tables III and IV, the vertical excitation energies of $d\text{-C}_4$ and $r\text{-C}_4$ are listed, respectively, together with the dominant electronic configuration of these states quoted at the equilibrium geometry of their respective ground states. At the CASSCF level of theory, the two lowest excited states of $r\text{-C}_4$ are triplets lying at 1.04 ($^3B_{1u}$) and 1.94 eV ($^3B_{2g}$) above the ground state, followed by two singlet states lying at 2.27 ($^1B_{1u}$) and 2.54 eV ($^1B_{2g}$), respectively. In Fig. 3 are given the CASSCF one-dimensional cuts of the 6D PESs of the electronic states of $r\text{-C}_4$, which are obtained by varying the R_{12} distance [cf. Fig. 3(a)] and the bending angle $\angle C_3C_1C_4$ [cf. Fig. 3(b)], where the remaining internal coordinates are kept fixed at $\angle C_3C_1C_4=116^\circ$ and $R_{12}=1.4312\text{ \AA}$ corresponding to the reference planar geometry. In Table III, our results for the singlet states [2.27 ($^1B_{1u}$), 2.54 ($^1B_{2g}$), and 3.41 eV (1A_g)] are compared with those of Ref. 11 (2.14, 2.23, and 3.45 eV). In Fig. 4, the CASSCF energy variations of the five lowest states of $d\text{-C}_4$ are presented. They are given along the bond distance R_3 [Fig. 4(a)], the bond distance $R_1=R_2$ [Fig. 4(b)], and the torsional angle τ [Fig. 4(c)]. Figure 4(c) shows the existence of a minimum for $\tau=0^\circ$ for the ground electronic state of $d\text{-C}_4(X^1A_1)$. The upper states should be planar also or possess small potential barriers to linearity.

Some general trends are found: A high density of electronic states is remarkable even for very low internal energies for the three isomers of C_4 . Such high density of electronic states is favoring their mutual interactions via Renner-Teller couplings (for $l\text{-C}_4$), vibronic and spin-orbit couplings (for three of them), and Jahn-Teller couplings (for the upper states of $d\text{-C}_4$). The conical intersections between the elec-

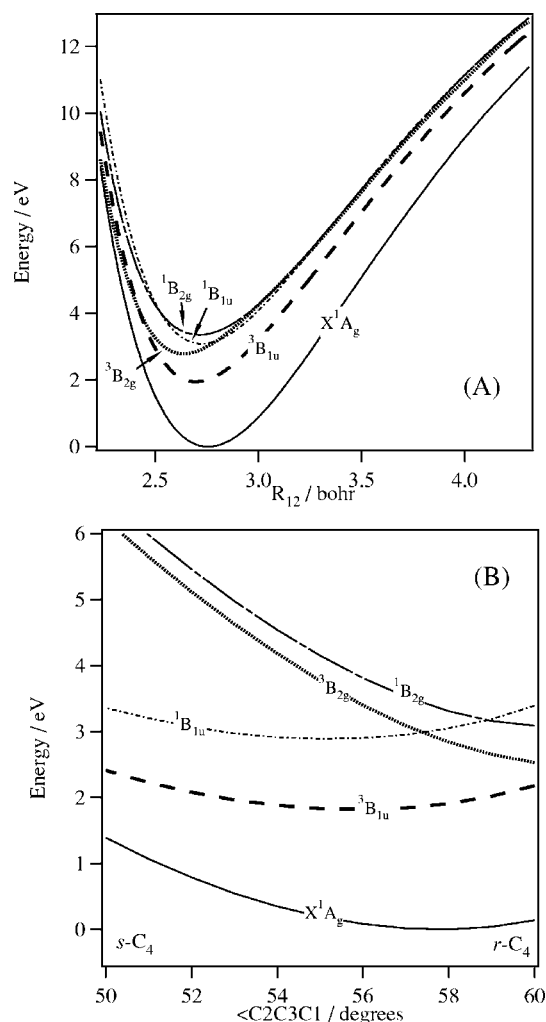


FIG. 3. CASSCF one-dimensional cuts of the lowest singlet and triplet electronic states of $r\text{-C}_4$ along the R_{12} stretch (A) and along the $\angle C_2C_3C_1$ in-plane angle (B). $s\text{-C}_4$ corresponds to the four member squared form of C_4 . The remaining coordinates are set to their reference values ($R_{12}=1.4314\text{ \AA}$, $R_{13}=1.5171\text{ \AA}$). These curves are given in energy with respect to the X^1A_g minimum.

tronic states having the same spin multiplicity are expected to occur, leading to avoided crossings in the C_1 point group [e.g., the crossing between $d\text{-C}_4(^3A_2)$ and the $d\text{-C}_4(^3B_1)$ states close to their equilibrium geometries, cf. Fig. 4(a)]. Finally, spin-orbit interactions should take place between the singlets and the triplets, and the triplets and the quintets in their mutual crossing regions. The isomerization processes can take place for high internal energies, converting one form to the other. All these interactions are mixing the wave functions of the electronic states of C_4 , complicating so the mapping of their 6D PESs. The assignment of the corresponding spectra is viewed to be quite complicated.

For illustration, we propose in the following an interpretation for the absorption spectrum of $l\text{-C}_4$ in the 25 000–35 000 cm^{-1} energy range, covering the $^3\Sigma_u^- \leftarrow X^3\Sigma_g^-$ excitation transition. This spectrum was measured by the group of Maier and it is given in Ref. 17. It shows sharp bands up to 40 000 cm^{-1} . The bands are broad because of shortening of the lifetime of the corresponding vibronic levels. Figure 5 presents the potential curves of $l\text{-C}_4$ elec-

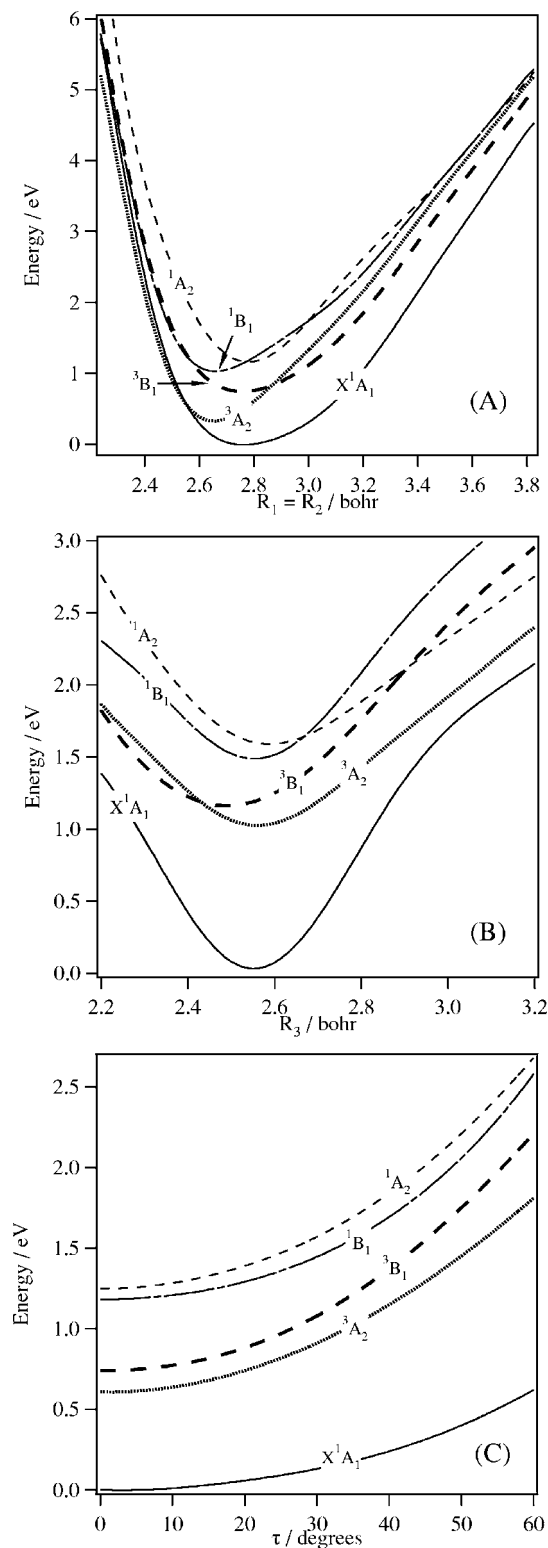


FIG. 4. CASSCF one-dimensional cuts of the lowest singlet and triplet electronic states of *d*-C₄ along the R_1 stretch (A), the R_3 stretch (B), and the dihedral angle τ (C). The remaining coordinates are kept fixed at their reference values ($R_1=R_2=1.4845$ Å; $R_3=1.3203$ Å; $\theta_1=\theta_2=152.6^\circ$). These curves are given in energy with respect to the X^1A_1 minimum.

tronic states in the vicinity of the $^3\Sigma_u^-$ state. This figure shows that the crossing between the $^5\Sigma_g^+$ and the $^3\Sigma_u^-$ electronic states is occurring almost for internal energies where the change of the shape of the bands in the absorption spectrum of Maier is detectable. Hence, we are expecting that the high

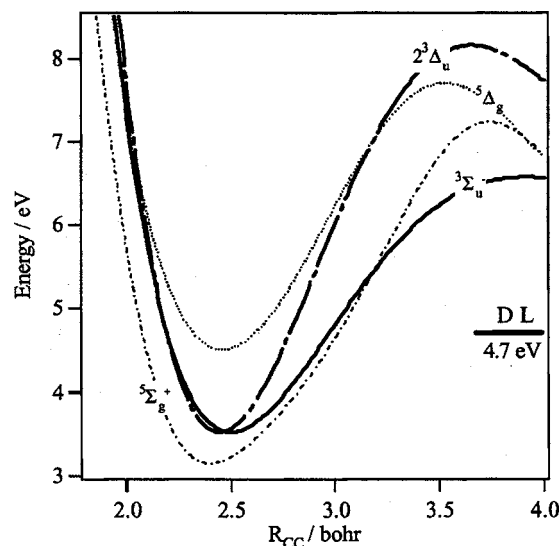


FIG. 5. Interactions between the triplet and the quintet states of *l*-C₄ in the vicinity of the $^3\Sigma_u^-$ state. DL denotes the first dissociation limit of *l*-C₄ [i.e., $C_2(X^1\Sigma_g^+) + C_2(X^1\Sigma_g^+)$].

vibrational levels of the $^3\Sigma_u^-$ state (i.e., located above this crossing) are predissociating to the first dissociation limit (denoted as DL in this figure) perhaps after interaction with the quintet state, thus reducing their lifetimes. Spin-orbit couplings, vibronic interactions, and Renner-Teller effects occurring for linear, planar, and nonplanar configurations should also play a role during this predissociation process before and/or after spin-orbit interactions. A complex multi-step mechanism is expected for the $l\text{-C}_4(^3\Sigma_u^-) \rightarrow C_2(X^1\Sigma_g^+) + C_2(X^1\Sigma_g^+)$ reaction.

V. CONCLUSIONS

In the present work, structural data of the lowest isomers and excited states of C₄ are reported using accurate *ab initio* methods and large basis sets. Our calculations confirm the existence of a linear form (*l*-C₄) and a rhombic isomer (*r*-C₄) and reveal the existence of a third isomer of C_{2v} symmetry (*d*-C₄). For these three isomers, a high density of electronic states is observed even for low internal energies, favoring their mutual interactions. Spin-orbit, Renner-Teller, Jahn-Teller, and vibronic couplings, in addition to isomerization processes, are expected to mix the rovibronic wave functions of the electronic states of C₄.

ACKNOWLEDGMENTS

This work has been supported by the Ministerio de Ciencia y Tecnología of Spain, Grant Nos. AYA2002-02117 and AYA2005-00702. Parts of this work have been done on the computers of CINECA (Bologna, Italy) and NERSC (UC Berkeley). The authors thank the staff of CINECA for their collaboration. One of the authors (M.L.S.) wants to acknowledge Professor Ricardo Tarroni for his help.

¹A. E. Douglas, *Nature (London)* **269**, 130 (1977).

²A. Van Orden and J. Saykally, *Chem. Rev. (Washington, D.C.)* **98**, 2313 (1998).

³J. Cernicharo, J. R. Goicochea, and Y. Benilan, *Astrophys. J.* **580**, L157 (2002).

- ⁴M. Algrananti, H. Feldman, D. Kella, E. Malkin, E. Miklazky, R. Naaman, Z. Vager, and J. Zaifman, *J. Chem. Phys.* **90**, 4617 (1989).
- ⁵D. Kella, D. Zaifman, O. Heber, D. Majer, H. Feldman, Z. Vager, and R. Naaman, *Z. Phys. D: At., Mol. Clusters* **26**, 340 (1993).
- ⁶W. R. M. Graham, K. Dismuke, and W. Weltner, *Astrophys. J.* **204**, 301 (1976).
- ⁷H. M. Cheung and W. R. M. Graham, *J. Chem. Phys.* **91**, 6664 (1989).
- ⁸L. N. Shen, P. A. Withey, and W. R. M. Graham, *J. Chem. Phys.* **94**, 2395 (1991).
- ⁹J. R. Heath and R. J. Saykally, *J. Chem. Phys.* **94**, 3271 (1991).
- ¹⁰C. Liang and H. F. Shaeffer III, *Chem. Phys. Lett.* **169**, 150 (1990).
- ¹¹M. Mühlhäuser, G. E. Froudakis, M. Hanrath, and S. D. Peyerimhoff, *Chem. Phys. Lett.* **324**, 195 (2000).
- ¹²D. Forney, P. Freivogel, M. Grutter, and J. P. Maier, *J. Chem. Phys.* **104**, 4954 (1995).
- ¹³D. Forney, J. Fulara, P. Frevogel, M. Jakobi, D. Lessen, and J. P. Maier, *J. Chem. Phys.* **103**, 48 (1995).
- ¹⁴P. Frevogel, J. Fulara, M. Jakobi, D. Forney, and J. P. Maier, *J. Chem. Phys.* **103**, 54 (1995).
- ¹⁵P. Frevogel, M. Grutter, D. Forney, and J. P. Maier, *Chem. Phys. Lett.* **249**, 191 (1996).
- ¹⁶H. Linnartz, O. Vaizert, T. Motylewsky, and J. P. Maier, *J. Chem. Phys.* **112**, 9777 (2000).
- ¹⁷M. Jungen and R. Xu, *Z. Phys. Chem.* **217**, 205 (2003).
- ¹⁸C. Xu, G. R. Burton, T. R. Taylor, and D. M. Neumark, *J. Chem. Phys.* **107**, 3428 (1997).
- ¹⁹J. D. Watts, J. Gauss, J. F. Stanton, and R. J. Bartlett, *J. Chem. Phys.* **97**, 8372 (1992).
- ²⁰P. J. Knowles, C. Hampel, and H.-J. Werner, *J. Chem. Phys.* **99**, 5219 (1993); **112**, 3106(E) (2000).
- ²¹H.-J. Werner and P. J. Knowles, *J. Chem. Phys.* **82**, 5053 (1985); P. J. Knowles, and H.-J. Werner, *Chem. Phys. Lett.* **115**, 259 (1985).
- ²²H.-J. Werner and P. J. Knowles, *J. Chem. Phys.* **89**, 5803 (1988).
- ²³P. J. Knowles and H.-J. Werner, *Chem. Phys. Lett.* **145**, 514 (1988).
- ²⁴MOLPRO, a package of *ab initio* programs designed by H.-J. Werner and P. J. Knowles, see <http://www.molpro.net> for more details.
- ²⁵T. H. Dunning, *J. Chem. Phys.* **90**, 1007 (1989).
- ²⁶R. Linguerr, I. Navizet, P. Rosmus, S. Carter, and J. P. Maier, *J. Chem. Phys.* **122**, 034301 (2005).
- ²⁷S. J. Blanksby, D. Schröder, S. Dua, J. H. Bowie, and H. Schwarz, *J. Am. Chem. Soc.* **122**, 7105 (2000).
- ²⁸Unpublished.
- ²⁹P. Botschwina, *J. Mol. Spectrosc.* **186**, 203 (1997).
- ³⁰J. M. L. Martin, D. W. Schwenke, T. J. Lee, and P. R. Taylor, *J. Chem. Phys.* **104**, 4657 (1996).
- ³¹D. W. Arnold, S. E. Bradforth, T. N. Kitsopoulos, and D. M. Neumark, *J. Chem. Phys.* **95**, 8753 (1991).